JOURNAL OF MATERIALS SCIENCE 12 (1977) 1–27

Review
Fast ion conduction materials

P. MCGEEHIN, A. HOOPER
Materials Development Division, AERE, Harwell, Didcot, Oxon, UK

A brief phenomenological introduction to the important physical parameters involved in ionic conduction in solids is followed by order of magnitude estimates of these quantities for materials which can be considered to be fast ion conductors. Experimental techniques are outlined, and a comprehensive compilation of currently available data on fast ion conductors is presented. The conductivity and diffusion data are coupled with additional criteria to indicate broad classes of materials which may show enhanced ion conductivity.

1. Introduction

The property of fast ion conduction (FIC) in solids is now well established, and it is found in diverse groups of compounds. Such materials can have important technological applications, extending and superseeding those areas traditionally reserved for liquid electrolytes. A growing emphasis on energy conservation and alternative energy sources has led to a good deal of research, especially to find better materials for battery and fuel cell applications. These must be relatively inexpensive, easy to fabricate, have good mechanical strength, high chemical stability, and most importantly, show FIC at near ambient temperatures. With these ideas in mind, the research effort in this area has increased quite dramatically over the last few years. However, no new materials with immediate technological applications have emerged, but much of the work has indicated which kinds of structures deserve further attention. The more fundamental aspects of FIC are also being examined in greater depth. Inevitably, some of the attention has been focused on the β-alumina compounds because of the immediate potential of the sodium compound as solid electrolyte in the sodium–sulphur battery.

The study of fast ionically conducting materials is confused generally by the dearth of understanding of their basic properties and the difficulty of performing adequate experimental tests on a wide range of compounds. The purpose of this review is, therefore, to establish the background for the study of fast ion conduction, including a compilation of the available data, in the hope that it may stimulate others to join a fast moving area of science bridging the disciplines of solid state chemistry and physics, and also encourage those already at work in the field. A brief introduction to ionic conductivity and diffusion is followed by an extension to the idea of FIC. General definitions of "fast" ion conductors in terms of the values of the conductivity, diffusion coefficients and activation energies are proposed. Common experimental techniques are also outlined, and the major part of the review comprises a materials survey in which the classification is based on the identity of the mobile species. The present review contrasts with those recently published by Huggins [1] and Steele and Dudley [2], essentially discussing FIC from a phenomenological viewpoint and attempting to provide a comprehensive compilation of currently available data.

2. General theory [3–5]

The ability of a material to allow the movement of ions through it can be gauged most readily from a combination of conductivity data, diffusion data, and motional narrowing of nmr lines, although the exchange of ions from aqueous or molten salts is sometimes used as an additional qualitative guide. The ionic conductivity of a solid,

σ, can be measured using a.c. or d.c. techniques with ionically blocking or conducting electrodes at two, three or four points of contact. Analysis of the results, particularly for a.c. measurements, needs careful attention in order to separate electrode and electrolyte effects, and also the influence of grain boundaries in polycrystalline material. The use of complex admittance or impedance plots is gaining acceptance in these respects. The ionic conductivity usually follows an equation of the form:

$$\sigma = (\sigma_0/T)\exp(-E_A/kT) \quad (1)$$

and the objective of all the experiments is to determine the overall magnitude of the conductivity, and E_A, the activation energy for ionic motion. The results are plotted as a graph of the logarithm of the product σT versus reciprocal temperature, and the activation energy can be determined from the slope of the resulting straight line. Occasionally the material under investigation shows conductivity by more than one ion, or perhaps also electronic conductivity, and in these cases it is necessary to determine the transport number, t, for each species: t measures the proportion of the total current being carried by each conducting species.

For simple ionic conductors in which current is carried by only one ionic species, the conductivity can be described by

$$\sigma = N.ze.\mu \quad (2)$$

where N is the number of mobile particles per unit volume, μ their mobility (drift velocity in unit electric field), and ze their charge. Simple thermodynamic arguments show that if current is carried via the creation of lattice defects, N will depend exponentially on reciprocal temperature, and if the actual migration process involves an activated state, so will μ. The derivation of Equation 1 from Equation 2 follows quite readily from these considerations, but this merely illustrates how the simplicity of Equation 1 obscures a great deal of information. Since ze varies little from one ion to another, the crucial factors influencing σ are N and μ.

The diffusion coefficient D is the constant which relates the diffusion flux J to the driving concentration gradient. Fick's law of diffusion may be written as

$$\mathbf{J} = -D\nabla c \quad (3)$$

where D is a measure of the ease with which thermally activated ions move through a lattice. The temperature dependence of D has the general form:

$$D = D_0\exp -E'_A/kT \quad (4)$$

where E'_A is the activation energy for the diffusion process. Clearly, if diffusion and conductivity proceed by the same mechanism and $t_{ion} = 1$, E'_A will approximately equal E_A in Equation 1.

Diffusion coefficients are most commonly determined by radiotracer analysis. If the system under investigation is at chemical equilibrium throughout the process then D_{tracer} equals the true self diffusion coefficient (D^*_T) of the diffusing species. This is also true for isoconcentration diffusion of foreign species. For a non-equilibrium situation D_{tracer} is known as the chemical diffusion coefficient ($\tilde{D}_T$). The theoretical expression for D from the viewpoint of random jumps of the diffusing species is $D = \Gamma r^2/6$ where Γ is the jump frequency and r the jump distance. However, the expression for D^*_T contains a factor f such that

$$D^*_T = \tfrac{1}{6}\Gamma_T r_T^2 f. \quad (5)$$

f is known as the "correlation factor" and is a measure of the extent to which successive jumps are related to one another. For a truly random situation $f = 1$.

A diffusion coefficient D_q may be calculated from conductivity data via the Nernst–Einstein Relation,

$$\sigma/D_q = Ne^2/kT. \quad (6)$$

Following Equation 5, D_q may be expressed as

$$D_q = \tfrac{1}{6}\Gamma_q r_q^2. \quad (7)$$

Here the mobile current carriers are lattice defects and f_q equals unity since their motion is random. The ratio D^*_T/D_q is commonly called the "Haven Ratio" (H_R) and from Equations 5 and 7:

$$H_R = \frac{\Gamma_T r_T^2}{\Gamma_q r_q^2}\cdot f. \quad (8)$$

In addition to the correlation factor, H_R contains a term which is determined by the particular mechanism of diffusion. Indeed a given mechanism or combination of mechanisms leads to unique values of H_R and thus experimental determinations or its value are of considerable diagnostic value in identifying the mechanism operating in any particular case. It should be remembered that

neutral defects will contribute to D_T^* but not to D_q and thus H_R will be larger than in their absence. Also H_R will be anomalously small in the presence of any electronic conductivity. In the case of the best ionic conductors, where the sublattice of the conducting species can often be regarded as being essentially liquid-like (i.e. where there is a relatively large number of "defect" sites to which each moving ion can jump), the distinction between diffusion coefficients should become unnecessary, and in any event, if only diffusion data are available, a rough idea of the conductivity can be gauged from Equation 6 assuming $H_R = 1$. Reference [126] contains a more detailed discussion of fast ion diffusion.

2.1. Values of σ, D and E_A for fast ion conductors

For a material to be classified as a fast ion conductor it should have an activation energy for conductivity and diffusion of ~ 0.1 eV (~ 2.5 kcal mol^{-1}, ~ 10 kJ mol^{-1}), i.e. about one tenth the energy needed to form a point defect in a relatively close packed ionic solid. The resulting shallow negative slope of the σ, D versus $1/T$ plots mean that D_0 and σ_0 (diffusion and conductivity at infinite temperature) will have values of 10^{-4} to 10^{-5} cm^2 sec^{-1} (D_0) and $10 - 1\ \Omega^{-1}$ cm^{-1} (σ_0). Corresponding room temperature values would be $D \sim 10^{-6}$ cm^2 sec^{-1} and $\sigma \sim 10^{-2}\ \Omega^{-1}$ cm^{-1}, with acceptable values one or two orders of magnitude lower than these. Some materials with ions which move with activation energies nearer the defect formation energy have much larger D_0 and σ_0, relatively high conductivities at high temperature, but lower D and σ at room temperature, e.g. oxygen transport in stabilized zirconia, sodium in NaCl. In the latter material $\sigma \sim 10^{-3}\ \Omega^{-1}$ cm^{-1} at 800°C, $\sigma_0 \sim 10^6\ \Omega^{-1}$ cm^{-1} and $E_A \sim 1.86$ eV whilst D_0 for $Na^{22} \sim 10$ cm^2 sec^{-1} and $E_A \sim 2.0$ eV [40]. Whilst the diffusion coefficient in FICs reaches the maximum values expected from simple calculations assuming every attempt is successful [1] implications of the low value of σ_0 found in FICs can be considered. Using the normal random walk formulation for defect transport outlined above, Huggins [1] derives

$$\sigma = \frac{C\beta r^2 \Gamma \alpha (ze)^2}{kT}, \qquad (9)$$

where C is the concentration of mobile ions, β the defect concentration i.e. the fraction of unoccupied mobile ion sites, defining the fraction of this species that is free to move, and α is a geometric factor which is the reciprocal of the number of possible jump directions from a given site ($\alpha = \frac{1}{6}$ for a close packed cubic lattice as above). Of the terms in Equation 9, C, r, α and ze do not vary by the required orders of magnitude from material to material, leaving only β and Γ to account for the low values of σ_0. In normally defective solids,

$$\beta = \exp - \Delta G_F / kT \qquad (10)$$

where ΔG_F is the free energy of formation of the intrinsic defect pair. However, in FIC solids β is found to be both temperature independent and much larger than for solids obeying Equation 10. Hence Γ; the jump frequency provides the only explanation. We may write

$$\Gamma = \Gamma_0 \exp - \frac{\Delta G}{kT} = \Gamma_0 \exp \frac{(\Delta S)}{k} \exp - \frac{E_A}{kT}, \qquad (11)$$

where ΔG is the free energy and E_A the enthalpy (activation energy) for migration, with ΔS the associated entropy. The significant terms are Γ_0 and ΔS. ΔS is not known for FICs, but it is reasonable to assume that it will be small since the mobile ion sublattice is generally highly disordered, and motion of ions will not significantly increase this disorder. Γ_0, the attempt frequency for a jump, must also be smaller than for normal solids, i.e. the phonon spectrum of the mobile ions in FICs is scaled towards lower frequencies. Some significant lattice dynamics experiments confirming the latter are outlined in the following section.

In Fig. 1 the variation of the conductivity of ions in a few FIC and other compounds is plotted against reciprocal temperature. The region of major interest for large scale technological applications of these materials is delineated in the top right-hand corner. It is within this region that the conductivity of liquid electrolytes is typically found. A 4M aqueous solution of NaCl has conductivity slightly larger than and activation energy close to that of $RbAg_4I_5$, as does the concentrated sulphuric acid electrolyte found in the lead–acid battery. Molten salt electrolytes also fall in this range, with activation energy generally smaller. This comparison with liquid electrolytes allows a fruitful analogy to be drawn, in which the sublattice of the mobile ion in FIC compounds is

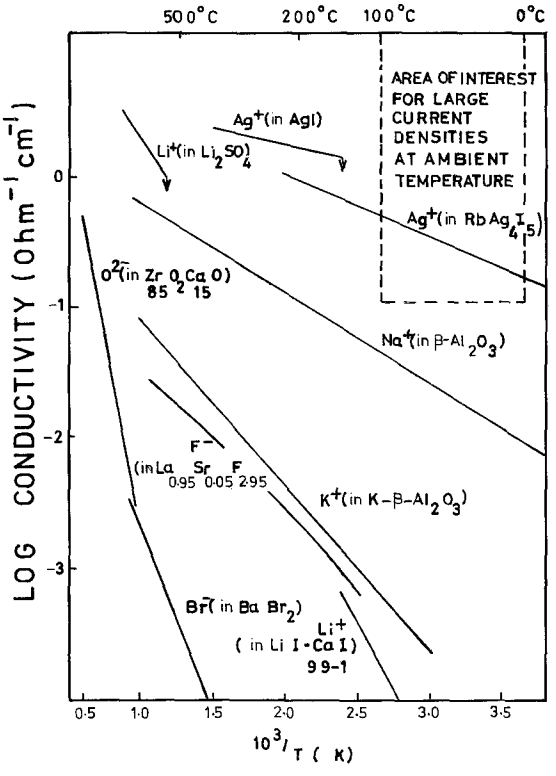

Figure 1 Typical ionic conductivity plot for a variety of materials. After reference [5].

regarded as liquid-like, with the other atoms in the crystal providing an essentially rigid network through which the mobile ions move.

3. Experimental methods

The major techniques which have been employed either in the selection or study of fast ion conductors are:

(1) Electrical:
  (a) a.c. (i) conductivity [6–10]
    (ii) dielectric loss [11–14]
  (b) d.c. (i) conductivity [15–16]
    (ii) polarization cell measurements [17, 18]
    (iii) pulse methods [19]
(2) nmr/epr [20–23]
(3) Neutron diffraction [24]
(4) X-ray diffraction [25–27]
(5) Optical/infra-red spectroscopy [28–31]
(6) Tracer diffusion [11, 12].

Each of the above has its own particular advantages and disadvantages, and the choice of method depends largely on the type of information required. However, as interest in FIC materials increases, more subtle experimental techniques are being used to obtain detailed information about lattice dynamics, mobile ions site occupancy, elastic constants etc. For example, Allen and Remeika [28] made direct measurement of the attempt frequency in beta-aluminas using far-infra-red techniques, whilst the dynamics of the onset of disorder in solid electrolytes and elastic constants have been studied using Raman and Brillouin light scattering [30]. Elastic constants have also been measured by inelastic neutron scattering [130]. Diffuse [131] and quasi-elastic [132] neutron scattering have been applied to silver iodides. X-ray diffraction studies have yielded information on anharmonic vibration of mobile ions. [27] and mobile ion site occupancy [25, 26, 133], whilst X-ray diffuse scattering has given information on ion-ion correlations in beta aluminas [134]. Ultrasonic attenuation due to mobile ions has also been studied [135]. Of the more common techniques used to identify good ionic conductors in programmes aimed at new materials, nuclear magnetic resonance and a.c. conductivity are extensively applied. They are discussed at greater length in the following two sections.

3.1. Nuclear magnetic resonance

As a guide to possible translational motion of ions in a solid which have nuclei with magnetic moments, motional narrowing of nmr absorption lines can be studied [125]. In the absence of motion of the nuclei the absorption line is broadened by anisotropic magnetic dipole and electric quadrupole interactions. These are averaged to much smaller values when the jump rate of the nucleus exceeds the frequency width of the "rigid lattice" nmr line (~ 10 kHz). At about the same jump rate there is an increase in the efficiency of the nuclear spin-lattice relaxation, resulting in a minimum of the characteristic relaxation time T_1. T_1 can be measured using pulse techniques by which it is also possible, within a limited range, to measure D directly. Routine nmr measurements do suffer, however, from the disadvantage that they do not unambiguously indicate the presence of translational motion, since non centro-symmetric rotation and rattling of the nucleus in the lattice gives rise to the same effects. However, the activation energy for such movement will typically be lower than for the translational motion involved in diffusion or conductivity.

3.2. Alternating current conductivity

In theory, a.c. measurements remove the need for electrodes reversible to the ionic species of interest by eliminating interfacial effects at sufficiently high frequencies. Particularly for the case of superionic conductors, however, this procedure is not always straightforward and a more complicated method of analysis may be needed to convert the generally frequency dependent a.c. response which is observed experimentally into meaningful bulk parameters, e.g. ionic conductivity. Complex plane plotting provides a method of representing the observed a.c. response in such a way that it may be analysed in terms of an $R-C$ network, each component of which will be linked to a particular atomic process or mechanism within the assembly. These fall basically into either interfacial or bulk microstructural phenomena. This type of analytical technique has been used by electrochemists for over 30 years in the study of liquid electrolytes [32], but has only recently been adopted for the study of solid-state systems [33–38]. It involves the plotting of the real and imaginary parts of a complex electrical quantity against one another as a frequency dispersion, the most common types of plot being categorized below.

Name	Symbol	Real	Imaginary
Impedance	Z^*	R_s	$-1/\omega C_s = 1/Y^*$
Admittance	Y^*	G_p	ωC_p
Permittivity	E^*	C_p	$-G_p/\omega = Y^*/i\omega$
Modulus	M^*	$1/C_s$	$\omega R_s = 1/E^* = i\omega Z^*$

G_p, C_p, R_s and C_s are the equivalent parallel or series components as measured by the usual type of experimental apparatus, e.g. bridge circuits.

For the case of ideal finite R and C, such diagrams consist of a combination of semi-circles and vertical straight lines, the peak positions and intercepts of which are simply related to the appropriate network components. The introduction of non-finite or non-ideal components such as Warburg type impedances or lossy capacitors, causes distortions in the plots and the presence of similar value components in the network will make the individual elements of the plots less distinct. Above a certain complexity many equivalent circuits may have similar complex plane plots and the choice of the appropriate circuit may be made easier by consideration of the known physical properties of the experimental assembly. For example, essentially parallel circuits may be eliminated if several processes are known to be working in series. The assignment of individual components to particular physical processes may be aided by a variation of sample geometry since, for example, bulk and interfacial effects vary as distinct functions of sample area and length. A unique interpretation of the type of processes which are occurring (i.e. dominating) cannot easily be made. The choice of which type of plot to use in a given circumstance is essentially determined by the ease with which the information can be extracted, but in the general case care must be taken when using only one type of plot. This is because each type of representation will highlight a particular range of the dispersion and it is possible to lose valuable information in a truncated range of frequency by the use of an inappropriate plot.

4. Preliminary survey of materials

In a recent publication on fast ion transport in solids [4], over 300 different compounds or classes of compounds were listed. Interest was principally focused on group I of the Periodic Table, since almost one quarter of the compounds contained mobile alkali metal ions (group IA), whilst a sixth were silver conducting compounds (group IB). Experimental conductivity of diffusion data were only presented for 80 compounds. Of these, approximately one half exhibited metallic or semi-conducting electronic conductivity (mainly transition metal oxides with overlapping d-orbitals), leaving approximately 40 electronically insulating compounds with measured ionic conduction parameters. In this final group, few compounds exhibit fast ion conduction as defined above, but of the 26 compounds with $\sigma > 10^{-3}$ Ω^{-1} cm^{-1} (or $D > 10^{-6}$ cm^2 sec^{-1}) at room temperature, 15 were silver conducting compounds, 4 were copper conductors (same group as silver in the Periodic Table), and the remaining 7 were alkali ion conductors. Only the silver compounds have conductivities approaching the truly fast (i.e. liquid-like) limit. In direct contrast to the listed compounds which have been examined experimentally, several others were considered to be potential fast-ion conductors. The criteria used to anticipate the behaviour of these materials will be discussed later, but it is worthwhile commenting that of the 30 or so compounds falling into this category, 16 compounds have active ions in group

IB of the Periodic Table, and 12 in group IA. Apart from zirconia, which exhibits O^{2-} ion conduction, no other materials are mentioned as fast anionic conductors. This is not surprising, however, because the larger anions will not be able to move as freely as the cations. Indeed, it is usually the anions which, in the best ionic conductors, contribute to the rigid atomic network through which the smaller cations readily diffuse.

From this superficial survey it is possible to draw two conclusions. Firstly, fast ion transport in electronically insulating solids is more often anticipated than established. This indicates the need for careful experimental programmes. Secondly, it seems likely that ions in groups IA and IB will move most easily in crystalline solids. This latter point will be taken up in greater detail in subsequent paragraphs, but from the point of view of battery applications of solid electrolytes, the group IA ions will be most useful. Their low electronegativity means they have cell reactions with large emfs, consequently offering the possibility of batteries with large energy and power densities.

5. Silver and copper conducting compounds

In Table I some 33 silver ion conducting compounds are listed. Of these, only 7 are not compounds based on silver iodide, the classical fast ion conductor. Below 149° C silver iodide exists in several crystal modifications based on the zinc blende or wurtzite structures, both of which favour ionic diffusion by an interstitial mechanism via face sharing polyhedra. Although these β-phases have unexceptional ionic conductivities, a phase change occurs at 149° C which gives silver iodide anomalously high ionic conductivity: at the melting point of the α-compound (555° C), the ionic conductivity actually falls. Above the transition temperature the anions are placed in a b c c configuration, with two Ag^+ ions per unit cell statistically distributed over a large number of sites. Analysis of the conductivity of α-AgI has involved the concept of a liquid-like cation sublattice involving ions on three common types of lattice site. However, van Gool [55] regards this as unnecessarily restrictive, and suggests that many other sites are involved. At any event, he suggests that wherever the Ag^+ ions are located, they will distort the rigid anion sublattice in such a way as to produce some ordering over several lattice dimensions, giving rise to domains in which particular sites are preferentially occupied. His particular suggestion is a tetragonal domain structure, which is supported by the original X-ray data [56].

No matter what the detailed mechanism of ionic conductivity in α-AgI may be, many attempts have been made to stabilize the high conductivity phase at room temperature, by substitution. The largest proportion of compounds in Table I reflect this approach. Following Owens [44] these attempts can be broadly classified as follows:

(a) anion substitution using, for example, S^{2-}. PO_4^{3-}, $P_2O_7^{4-}$, SO_4^{2-}, WO_4^{2-},

(b) cation substitution giving rise to both the well documented MAg_4I_5 class of compounds with high conductivity over a wide temperature range around room temperature, and the organic ammonium iodide-silver iodide electrolytes. These latter compounds are double salts formed between tetra-alkylammonium iodides and silver iodide in mole ratio 1:6, or between polymethonium iodides and silver iodide in the ratio 1:12. Best values of Ag^+ conductivity are $\sigma \sim 10^{-2}\ \Omega^{-1}\ cm^{-1}$ at 25° C. A few typical compounds are listed in Table I, but there are a large number of others which have been investigated [44, 57]. Certain trends have been established, but these are not fully understood. Furthermore, like many of these Ag^+ compounds, they tend to be thermodynamically unstable. Similar work has been performed by Linford *et al.* [58] on silver sulphonium iodide systems such as $AgI\text{-}(CH)_3SI$, $AgI\text{-}(CH_2)_4SCH_3I$. Maximum conductivities fall in the range $3 \times 10^{-3}\ \Omega^{-1}\ cm^{-1}$ to $4 \times 10^{-2}\ \Omega^{-1}\ cm^{-1}$ at 25° C.

(c) mixed ion substituted silver iodide; these involving the ternary system $AgI \cdot HgI_2 \cdot Ag_2S$, with the latter compound replaced by Ag_2Se or Ag_2Te, and the compounds formed between AgI and the group IA cyanides. Conductivities are quite good, but stability is again a problem.

Also listed in Table I are a number of Cu^+ conducting compounds, which are mostly analogous to the corresponding silver compounds. They generally form the conducting phase at higher temperatures than their silver analogues, and conductivities are lower. In an investigation of a series of double salts of substituted organic ammonium halides with ring structures and cuprous halides, Sammells *et al.* [59] found room temperature conductivities in the range 10^{-2} to $10^{-3}\ \Omega^{-1}\ cm^{-1}$

TABLE I Silver and copper conductors

Compound	Range of stability of high σ form	Ionic conductivity (Ω^{-1} cm^{-1})	Activation energy (eV)	No. of dimensions of conductivity	Reference
AgCl	~150 – 430° C	8×10^{-5} at 200° C	~0.18	3	[41]
AgBr	~175 – 400° C	8×10^{-4} at 200° C	~0.15	3	[41]
αAgI	146 – mp 555° C	1 at 150° C	0.05	3	see [42]
αAg_2S	179° C –	3.8 at 200° C	0.05	3	
αAg_3SI	> 245° C	1 at 250° C	0.04	3	
βAg_3SI	< 235° C	0.1 at 200° C	0.17	3	
Ag_3SBr	< 300° C	2×10^{-3} at 25° C	0.23	3	
αAg_2Se	133° C –	3.6 at 220° C	~0.1	3	
αAg_2Te	150° C –	1 at 220° C	~0.1	3	
αAg_2HgI_4 *	51° C	10^{-3} at 60° C	0.36	3	
	51° C – 72° C	9×10^{-2} at 60° C	0.33	3	[43]
$Ag_4HgSe_2I_2$	No data available				[44]
$Ag_8HgS_2I_6^-$	< 20 – > 100° C	0.07 at 25° C			[44]
KAg_4I_5 †	– 136 – 253° C	0.12 at 20° C	0.07	3	[42]
$K_{0.75}Ag_{0.25}Ag_4I_5$	– 139 – ~200° C	0.12 at 20° C		3	[45]
$RbAg_4I_5$	– 155 – ~200° C	0.12 at 20° C	0.07	3	[42]
$NH_4Ag_4I_5$	Data unreliable			3	[46]
KCN. 4AgI	< 20 – > 150° C	0.14 at 25° C			[44, 47]
RbCN. 4AgI		0.18 at 25° C			[44, 47]
CsCN. 4AgI		0.0009 at 25° C			[44]
Ag_2SeO_4. 2AgI		0.002 at 25° C			[48]
$Ag_6I_4WO_4$		0.047 at 25° C	0.156		[47, 49, 50]
$Ag_7I_4PO_4$	< 25 – 79° C	0.019 at 25° C	0.165		[49, 50, 57]
$Ag_{13}(Me_4N)_2I_{15}$	> 50° C –	0.04 at 30° C	0.19	3	[53]
$Ag_{13}(Et_4N)_2I_{15}$		0.022 at 30° C	0.26	3	[53]
$Ag_{19}I_{15}P_2O_7$	< 25 – 147° C	0.09 at 25° C	0.143		[47, 49, 50]
$(CH_3)_4NAg_6I_7$	0 – 120° C	0.4 at 20° C	0.16	3	[42]
$(CH_3)_2(C_2H_5)_2NAg_2I_7$		0.06 at 22° C		3	[44, 45]
$(C_2H_5)_4NAg_6I_7$		0.01 at 22° C		3	[44, 45]
$(C_5H_5NH)Ag_5I_6$ ‡	< 200 – 400 K	0.13 at 50° C	(< 50° C ~ 0.5 (> 50° C ~ 0.21	3	[44, 51]
$Ag_7I_4AsO_4$	< 20 – > 100° C	0.004 at 25° C	0.174		[54]
$Ag_7I_4VO_4$	< 20 – > 100° C	0.007 at 25° C	0.174		[54]
$(C_5H_5NH)_5Ag_{18}I_{23}$	< 20 – > 100° C	0.008 at 25° C	0.21	2	[51, 52]
$AgAl_{11}O_{17}$ (silver β-alumina)	very stable	6.4×10^{-3} at 23° C	0.17	2	[12]
αCuBr	> 470° C	~0.3 at 470° C	small	3	see [42]
αCuI	> 407° C	~0.1 at 450° C	small	3	
αCuS	> 91° C	0.2 at 400° C		3	
(Cu deficient)		0.2 at 130° C	0.25	3	
αCu_2Se	> 110° C	0.1 at 210° C		3	
(Cu deficient)			0.12	3	
αCu_2HgI_4	> 767° C	10^{-5} at 67° C	0.60	3	

* Both Ag^+ and Hg^+ conduct: $t_{Hg} \sim 0.06$.

† Below 37° C begins to disproportionate slowly.

‡ Phase change at 50° C gives discontinuity in σT versus $1/T$ plots.

and activation energies for Cu^+ motion ranging between 0.12 and 0.29 eV. Lowest activation energy was for quinuclidine hydrobromide–CuBr (87.5 mol %) over the temperature range 50 to – 20° C.

The crystal structures of many of the compounds listed in Table I have been determined, and it has been possible to combine this information with the conductivity and activation energy data, allowing a few general features of all these compounds to be suggested. Principally, these compounds have:

(1) a large number of mobile ions (~ 10^{22} cm^{-3} in most cases);

(2) a large number of available sites for each mobile ion which have similar energy and approximately the same (low) co-ordination;

(3) a low potential barrier to the motion of the ions;

(4) structures with continuous chains of face-sharing octahedra and tetrahedra through which the ions can diffuse, mostly in three dimensions.

Clearly, these points must be borne in mind when considering other compounds as possible ionic conductors. Van Gool [55] and Armstrong *et al.* [42] have followed this procedure, particularly the latter for silver and copper compounds. Of the compounds which they consider deserve closer examination, concern about stability and potential applications must cast some doubt on their ultimate usefulness.

At this stage it is perhaps relevent to ask why silver, and to a lesser extent copper, form solid compounds with such unique properties. The above criteria indicate that the answer lies partially in the ability of these ions to form compounds in which they have low co-ordination number and flexible stereochemistry. The unhindered nature of these compounds allows the cations to move without colliding with other ions, and this ability also appears to be linked to their facility in polarizing other ions. The outer d-electrons provide ineffective shielding of the nuclear change, and so they readily attract electrons. This allows them to form bonds with covalent character at each intermediate position through which they move, thereby reducing the energy of this transition state. In this context it is pertinent to comment that the anions of these conducting solids are also important. Examination of Table I shows the majority of them to be highly polarizable; contrast the conductivities of AgCl and AgBr with that of AgI, which contains highly polarizable I^- ions.

Of the silver compounds listed in Table I which are not based on AgI, the other two silver halides are unexceptional, and have been included mainly for comparison purposes. Silver β-alumina will be discussed together with its alkali–metal analogues in a later section. The remaining compounds are formed between silver and the highly polarizable group VIB anions, illustrating again the importance of this concept.

In terms of potential applications, silver (and also copper) conducting compounds suffer from three main disadvantages. Firstly, as mentioned above, they tend to be unstable, or form highly conducting phases only at temperatures above ambient. Secondly, the emfs of cells involving Ag^+ and Cu^+ tend to be less than 0.7 V. This is a severe disadvantage when potential battery systems are considered. Finally, they are expensive for large scale, low technology applications.

6. Fast anionic conduction

Doped group IVA oxides give rise to high anionic conductivities. These compounds, ZrO_2, HfO_2, CeO_2 and ThO_2, have high oxygen conductivities when doped with either alkaline earth oxides, Sc_2O_3, Y_2O_3 or rare earth oxides [60]. Doping achieves two objectives. Firstly, in those materials which do not normally have the fluorite structure (ZrO_2 and HfO_2), the dopants stabilize this phase. Secondly, the presence of divalent or trivalent cations on the cation sublattice causes the formation of anion vacancies to preserve electrical neutrality. Oxygen conduction occurs principally via these vacancies. In Table II the electrical properties of the most common solid oxide

TABLE II Electrical properties of solid oxide electrolytes*

Electrolyte	% anion vacancies	Ionic conductivity at 1000° C (Ω^{-1} cm^{-1})	Activation energy (eV)
ZrO_2 + 12% CaO	6.0	0.055	1.1
ZrO_2 + 9% Y_2O_3	4.1	0.12	0.8
ZrO_2 + 10% Sm_2O_3	4.5	0.058	0.95
ZrO_2 + 8% Yb_2O_3	3.7	0.088	0.75
ZrO_2 + 10% Sc_2O_3	4.5	0.25	0.65
ThO_2 + 8% Y_2O_3	3.7	0.0048	1.1
ThO_2 + 5% CaO	2.5	0.00047	1.1
CeO_2 + 11% La_2O_3	5.0	0.08	0.91
CeO_2 + 15% CaO	7.5	0.025	0.75
HfO_2 + 8% Y_2O_3	3.7	0.029	1.1
HfO_2 + 12% CaO	6.0	0.004	1.4
La_2O_3 + 15% CaO	2.7	0.024	0.88

*Reprinted with permission from *Chemical Reviews* **70** (1970). Copyright by the American Chemical Society.

electrolytes are listed. Ionic conductivites at 1000° C are $\sim 0.1\ \Omega^{-1}cm^{-1}$ at best, and activation energies of ~ 1 eV are typical. The main applications of these materials are in the measurement and monitoring of oxygen activity, high temperature fuel cells, kinetic studies and thermodynamic property measurements. A possible development involves doping them with pentavalent compounds such as Ta_2O_5 or Nb_2O_5. Interstitial oxygen ions would probably result, and they may be mobile. However, it seems unlikely that the conductivity of these materials will exceed those of the oxygen deficient compounds.

Takahashi and co-workers [61–64] have studied Bi_2O_3 doped with SrO, CaO, La_2O_3, WO_3, Y_2O_3 and Gd_2O_3. In all cases, conductivities were markedly superior to the zirconia-based electrolytes, but concern about the ease with which the compounds form solid solutions casts a shadow on their ultimate usefulness. Table III lists some typical results. Up to $\sim 25\%$ dopant level there is a phase transformation between ~ 600 and 700° C, reminiscent of pure Bi_2O_3, when σ increases by about three orders of magnitude and approaches $\sim 1\ \Omega^{-1}cm^{-1}$ at 800° C. Above this level of doping (up to $\sim 50\%$) the conductivity varies continuously with temperature, but falls with increase in dopant. Activation energies in this range are ~ 0.8 ev. Only the low temperature forms of pure Bi_2O_3 and the low dopant WO_3 compound show appreciable electronic conductivity. Different dopants and the degree of doping give different crystal structures, but all structures contain oxygen vacancies. Another possible oxygen conducting compound is LaOF, which Kleitz [65] suggests may allow movement of oxygen by exchange of sites with fluorine ions. If this is the case, however, it seems reasonable to expect some F^- conductivity as well.

TABLE III Oxygen conductivities in doped bismuth oxides

Compound	Conductivities ($\Omega^{-1}cm^{-1}$)
$(Bi_2O_3)_{0.8}(SrO)_{0.2}$	6×10^{-3}(500° C), 2.5×10^{-2}(600° C), 2.2×10^{-1}(700° C)
$(Bi_2O_3)_{0.8\text{–}0.667}(WO_3)_{0.2\text{–}0.333}$	$\sim 10^{-1}$(730° C)
$(Bi_2O_3)_{0.75}(Y_2O_3)_{0.25}$	1.2×10^{-2}(500° C), 1.6×10^{-1}(700° C)
$(Bi_2O_3)_{0.65}(Gd_2O_3)_{0.35}$	$2 - 4 \times 10^{-2}$(600° C)
$(Bi_2O_3)_{0.9}(Gd_2O_3)_{0.1}$	4.5×10^{-2}(600° C)

Apart from oxygen, the only other anion to be consistently mobile is fluorine. Typical fluorides cannot really be regarded as fast ion conductors but in doped CaF_2, conductivities can approach $10^{-2}\Omega^{-1}cm^{-1}$ at 700° C, with activation energies ~ 1 eV. CaF_2 is interesting in that doping with NaF produces F^- vacancies, whilst doping with Y^{3+} leads to F^- interstitials, and both types of material have similar fluorine conductivities [66]. Further work in this area involves the use of higher YF_3 concentrations, possible use of YbF_3 as dopant, and investigations of the ternary system CaF_2–$CaYF_4$–NaF. Derrington and co-workers [67, 68] have studied the ionic conductivity of some alkaline earth halides with various structures and distinguish three classes of behaviour. For $MgCl_2$, $CaCl_2$, $CaBr_2$ and $BaBr_2$ there is an increase in conductivity of several orders of magnitude on melting, whilst $BaCl_2$ and $BrBr_2$ show a solid–solid transition accompanied by a large increase in conductivity with little subsequent change on melting. CaF_2, SrF_2, BaF_2 and $SrCl_2$ have continuous conductivity plots as solids, and σ changes very little on melting. However, at 700° C, $\sigma < 10^{-2}\Omega^{-1}cm^{-1}$ for all except $SrCl_2$ ($\sim 10^{-1}\Omega^{-1}cm^{-1}$) and $E_A \sim 2$ eV. These and other workers have studied lead halides, both pure and doped with potassium. For example KPb_3F_7 has a phase transition at 280° C and at ~ 300° C, σ is greater than $10^{-3}\Omega^{-1}cm^{-1}$ [69]. Some work has been done on a number of fluorides with tysonite-related structures (LaF_3, CeF_3, YF_3, ErF_3). Best amongst these is LaF_3 doped with 5% SrF_2, when $\sigma \sim 10^{-4}\Omega^{-1}cm^{-1}$ at room temperature, rising to $10^{-2}\Omega^{-1}cm^{-1}$ at 400° C [71]. Koryta [70] reports that the lanthanum fluoride solid electrolytes (and the silver halides) have been used in ion selective electrodes for inorganic chemical analysis. Applications of fluorine conducting electrolytes include the $Ca/CaF_2/NiF_2$, Ni battery which has an open circuit voltage of 2.78 V, offering potentially high energy densities. Mg can replace Ca as the anode material, whilst FeF_2 or CrF_2 can be used for the cathode [66].

Currently there is considerable interest in the possibility of finding solid electrolytes which conduct other anions, e.g. carbon, nitrogen and sulphur. These would be used in electrochemical probes for monitoring the elements in industrial processes. The materials depend very much on the exact nature of the application, but examples of those tried are Na_2CO_3/Li_2CO_3, BaC_2/BaF_2,

CaS/Y_2S_3 and AlN. Other possibilities may be found in some oxide systems (e.g. CaO exhibits high C diffusion).

7. Hydrogen conductors

Applications of hydrogen ion conductors are easy to envisage, and they would find immediate use in low temperature fuel cells, etc. However, few materials have been found which exhibit such conductivity. This is associated with the instability of the hydride ion, H^-, in all oxidizing environments, and the ease with which the small proton (H^+) is trapped. The hopping mechanism of proton conduction in aqueous systems has not so far been found in solids. Only a small amount of data is reported in the literature. Solid KHF_2, which in its low temperature α-modification exhibits protonic conduction has a conductivity of $\sim 10^{-7}\Omega^{-1}\,cm^{-1}$ at 196° C [72], the temperature at which it changes to the β-form. The α-phase has a tetragonal cell unit in which alternating layers of F–H–F dumb-bells and potassium ions occur perpendicular to the c-axis, whilst the β-phase has the same structural units in the cubic NaCl array. At 196° C the conductivity jumps by almost three orders of magnitude, but now 75% of the current is carried by F^- and 25% by K^+. The protonic contribution in this phase could be the same as in the α-phase. The ease with which hydrogen bonds are formed will naturally impede hydrogen mobility, but they can be the key feature in interesting structures which may exhibit ionic conduction. For example in KDP, KH_2PO_4, infinite three dimensional networks of PO_4^{3-} anions are joined to four neighbouring groups by hydrogen bonds between each oxygen atom on one group and one oxygen atom on each of the neighbours. All the hydrogen bonds in the lattice are involved in these bonds. The potassium ions reside in the interstices of the framework. Doping with a divalent anion such as SO_4^{2-} will form hydrogen or K^+ vacancies which may allow diffusion, whilst addition of, for example, PO_3^- may also allow the movement of hydrogen. $(NH_4)_2H_3IO_6$ has a similar structure [73]. Indeed, recent measurements [74] of proton mobilities in KDP doped with SO_4^{2-} and SiO_4^{4-} at the level of fractions of a mole percent give values of $\sigma_0 \sim 10$ and $E_A \sim 0.6$ eV (typically). Proton mobility has also been investigated in hydrogen tungsten bronzes of formula $H_{0.46}WO_3$, $H_{0.39}WO_3$ using pulsed nmr [75]. Activation energies of 0.14, 0.19 eV and correlation time pre-exponential factors of 69 and 47 n sec were obtained respectively.

8. Alkali ion conductors

The interest in materials which contain highly mobile alkali ions stems from their possible applications in solid-state battery systems and the like, which at the present time are of considerable technological interest. The highly electropositive alkali ions provide the possibility of large cell voltages and very high energy densities. In general terms, a particular material will be required to act as either an electrolyte or an electrode. Both applications require solids with a high ionic conductivity, preferable at ambient or relatively low temperatures. For an electrolyte material the restriction of low electronic conductivity must be added. A mixed conductor is suitable for electrode applications since it provides compatibility between the device (in which current is carried by ions) and the external electronically conducting circuit.

Data on alkali ion conductors is collected together in Table IV. Many of the compounds listed in Table IV have been selected for study using the criteria for FIC outlined above. Broadly they fulfil at least one of the requirements of (a) an open framework of ions within which the alkali ions can reside and (hopefully) move, and (b) an excess of available sites over the number of mobile ions actually present. The information presented in Table IV is largely the result of the rapid recent expansion in FIC research, and as such the experiments have been performed in a variety of ways, from the superficial level (as in materials screening surveys) to the extremely useful and thorough examination of just one particular compound. Generally, it is fair to conclude that the data presented here cannot be regarded as the last word on any of compounds studied, and that further and more detailed experiments will no doubt provide additional useful information. Furthermore, some of the compounds mentioned in Table IV may, in the pure form, have discouraging ionic conductivities which can be greatly enhanced by doping with other ions.

In the following two sections, some comments on the contents of Table IV are made, primarily with a view to outlining the major features. In Fig. 6, some of the data presented in Table IV is portrayed graphically, the shaded region being the area of prime technological importance.

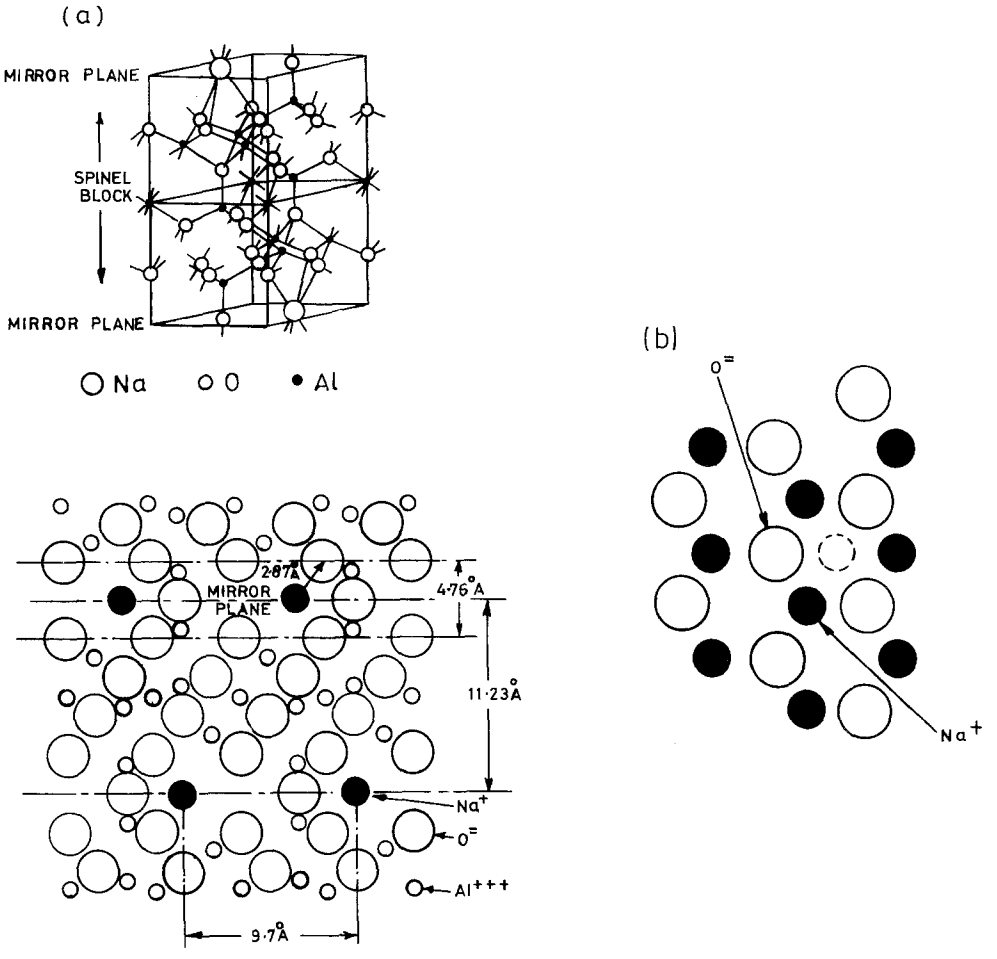

Figure 2 Crystal structure of beta-alumina (a) showing the spinel block (upper) and a section perpendicular to the mirror plane (lower), (b) showing a section in the mirror plane. The dotted circle shows one alternative sodium site.

8.1. β-alumina-type compounds

Compounds with the β-alumina type of structure have been extensively studied with particular reference to FIC. They have the general formula $M_2O.11\ Al_2O_3$ where M is an ion in group IA or IB of the Periodic Table. In the most commonly studied compounds M is Na or Ag, but all the isotypes are readily formed by ion exchange. The crystal structure (Fig. 2a), is basically hexagonal and shows a layered formation perpendicular to the *c*-direction. Blocks of aluminium and oxygen ions in a spinel-like configuration provide the main structure, but these are interspersed by layers containing oxygen and sodium* ions only. The spinel blocks are separated by Al–O–Al "pillars" and are mirrored in the Na–O plane. The spacing is such that motion of the Na ions is possible, in two dimensions within the layer. No motion is possible in the *c*-direction. The unit cell has a *c*-dimension of 22.6 Å and involves two spinel blocks related by a two-fold screw axis. Several modifications to the structure are found, the most common being that of β″-alumina ($M_2O.xAl_2O_3$: $x = \sim 5$ to 7). This has three spinel blocks in it's unit cell related by a three-fold screw axis. Any samples of "β-alumina" generally consist of a mixture of both the β and β″ phases, but the latter may be stabilized by the addition of, for example, MgO or LiO_2. This is advantageous in some respects since the ionic conductivity of the β″ phase is higher, but in many applications this has to be balanced against lower mechanical

*In sodium β-alumina $Na_2O.11Al_2O_3$.

strength. In the mirror plane of the unit cell of these structures the sodium ions can take up one of two possible positions (Fig. 2b). A study of the crystal structure indicates that these two sites are equivalent in β''-alumina but non-equivalent in β-alumina itself. In both cases there is insufficient sodium present in the structure to provide full occupancy of these sites and the transport properties are governed by the motion of the sodium ions by some form of interstitial or interstitialcy mechanism. Further and more detailed structural information will be found elsewhere [26]. Although the low site occupancy is a necessary condition for fast ion transport to occur it is not necessarily a sufficient one, and the precise mode of transport in β-alumina type materials is not well understood. In fact a study of the crystal structure particularly from an electrostatic viewpoint does not lead to the very low values of activation energy for motion which are observed. Several models have been put forward to explain FIC in these materials, notably the domain theory [76]. Sato and Kikuchi [77] discuss the problem in terms of vacancy mechanisms in a cation-disordered phase. They employ a mathematical path probability method. A purely phenomenological treatment of FIC is discussed in the free-ion model of Rice [78] (See also [127] and [128]). A particularly significant calculation on the high mobility in beta-alumina has been performed by Wang *et al.* [136]. They determine potential energy curves for various carrier ions taking into account Coulomb potential energy, the short range repulsive Born–Mayer potential, and the polarization energy. The energy difference between the two alkali ion sites in the mirror plane is found to be ~ 2 eV in stoichiometric crystals, but in (real) crystals, containing an alkali excess, the extra ions may form interstitialcy pairs whose in-phase motion has a potential energy barrier comparable to experimental activation energies. Attempt frequencies and pre-exponential factors calculated using this method also show good agreement with experiment.

Many workers have studied this type of material experimentally. In particular, the sodium form $Na_2O.\ xAl_2O_3$ has been prepared with a range of values of x, but most commonly with $x = 11$ (β) and $x = 5$ to 7 (β''). In these forms it has been prepared as single crystals and as polycrystalline compacts by both sintering and hot pressing [79]. The properties of the latter are strongly dependent on fabrication conditions. For preparation details see for example [80, 81]. β-alumina has been investigated using most of the techniques outlined in Section 2. Conductivity measurements have been made using both a.c. and d.c. techniques using either blocking platinum, silver or gold electrodes or reversible electrodes such as molten sodium or sodium salts, or solid bronze type structures. The highest reported conductivities for sodium beta alumina of 0.033 $\Omega^{-1}\,cm^{-1}$ [12] and $0.014\,\Omega^{-1}\,cm^{-1}$ [6] at 300 K were determined using single crystal samples with current flowing perpendicular to the c-axis. The former workers used indium electrodes at 1.5 MHz and reported no frequency dependence. In [6] reversible tungsten bronze electrodes were used at 10 kHz. Additional references which cover in some detail the many aspects of β-alumina type materials are [8, 11, 15, 19, 20–23, 29, 82–97]. The thesis of McGowan [88] contains 151 references to β-alumina and related topics.

In addition to the different forms of β-alumina materials, which include the replacement of sodium by Ag, Li, K, Sr, etc, there also exist materials in which aluminium is replaced by gallium and iron. β-gallia and β-ferrite both have the β-alumina structure and may also allow variable concentration of a number of different mobile ions. Little information is available for β-gallia, but in many ways its properties appear similar to β-alumina. Details of preparation of polycrystalline samples are given by Boilot *et al.* [22], who also measured the ionic conductivity using a four-point a.c. technique with platinum electrodes. They report a value of $3 \times 10^{-2}\,\Omega^{-1}\,cm^{-1}$ at 300° C and an activation energy of 0.25 eV. Chicotka [98] reports conductivity measurements on sintered β-gallia, $Na_2O.\ xGa_2O_3$, with x in the range 3.5 to 11. σ was frequency independent at greater than 10^5 Hz, and peaked in the range $5.5 < x < 6.5$. For $x = 6$, $\sigma = 0.14\,\Omega^{-1}\,cm^{-1}$ at 300° C, $E_A \sim 0.13$ eV. Single crystals of β-gallia have been grown using an NaF flux [99]. β-ferrite is unique in that it is also an electronic conductor, and so is a good candidate for electrode applications. In addition, it is relatively easy to change the proportion of alkali ions in the lattice. Dudley and Steele [100] have studied the ionic and electronic conductivity of K β-ferrite. The electronic conductivity and its activation energy vary with stoichiometry, and at 610 K, $\sigma_e = 1.5\,\Omega^{-1}\,cm^{-1}$, $\sigma_i = 2.3 \times 10^{-2}\,\Omega^{-1}\,cm^{-1}$. Generally, the

ionic conductivity compares with K β-Al_2O_3, but the electronic contribution is much greater.

8.2. Tunnel structures

The basic building block of a large number of tunnel structures is the octahedral configuration of oxygen ions around cations typically found in ReO_3 and TiO_2 (rutile) structures.

The ReO_3 structure is cubic, with the rhenium atom at the cube centre surrounded by six oxygen atoms arranged octahedrally at the face centres (Fig. 3a). A closely related structure is that of perovskite with the general formula ABO_3, e.g. $CaTiO_3$. Here element B replaces Re and two atoms of element A are added at the face-centred positions not occupied by oxygen (Fig. 3b). This structure is only stable for elements with ionic radii obeying the equation:

$$R_A + R_O = t\sqrt{2}\,(R_B + R_O) \text{ with } 0.9 < t < 1$$

and with ions of comparable size occupying A and O positions. In a great number of compounds with the perovskite structure, A is an alkali or alkaline earth ion, and B is a transition metal ion. The linking together of the oxygen octahedra surrounding B at their corners leaves the A atoms as interstitials in tunnels which run parallel to one of the cube axes. In ABO_3 all of the A sites are occupied, but series of nonstoichiometric compounds exist with a lower occupancy of A sites. These materials have the general formula $A_xB_yO_z$ $(0 < x < 1)$ where B_yO_2 $(x = 0)$ is the highest binary oxide of the element B and are known as "bronzes". The first compounds discovered with this structure were the tungsten bronzes (A_xWO_3). Their structure is intermediate between the AWO_3 perovskite and the WO_3 structures, the latter being a distorted (monoclinic) version of ReO_3 with the tungsten atom slightly off-centre and alternately long and short W–W bonds. The

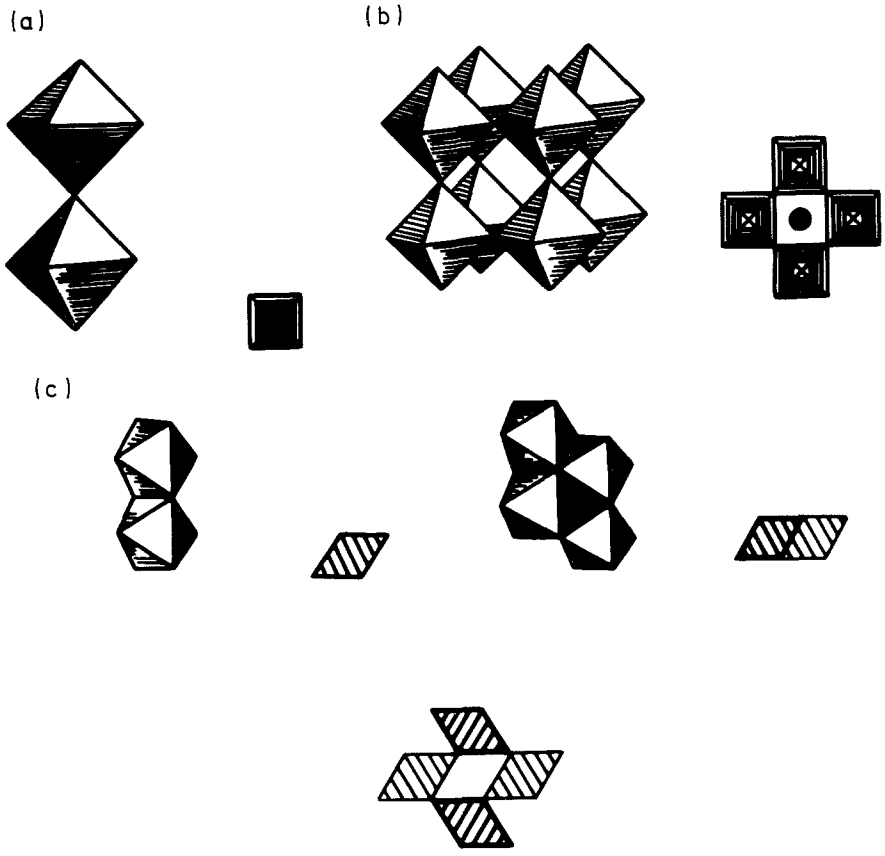

Figure 3 The structure of (a) ReO_3 (b) perovskite and (c) rutile. The octahedra have oxygen ions at their vertices and cations at the centres. Projections down the chains are also shown. In (c) the single and double rutile chains are illustrated as well as (lower) the rutile structure. Infinite lattices are generated by vertex sharing. After [129].

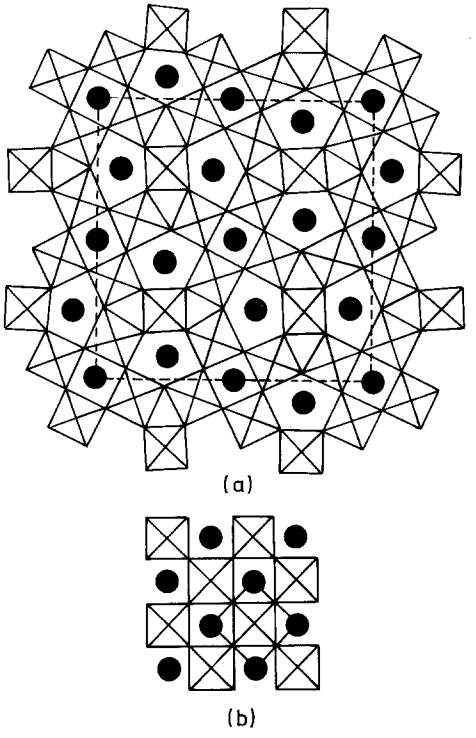

Figure 4 0 0 1 projections of tetragonal 1 and cubic tungsten bronze structures.

symmetry of the crystal structure decreases with the value of x and passes from cubic, through tetragonal, to monoclinic and orthorhombic forms. Hexagonal structures have also been described. All the structures are based on the linking of WO_6 octahedra by corner sharing, but the particular structure adopted in each case is also controlled to a considerable extent by the ionic radius of A. This size constraint is not found in the vanadium bronzes $A_xV_2O_5$. The way in which the octahedra may link is shown in the illustration of the cubic tetragonal bronze structures (Fig. 4). In the cubic form, rings of four octahedra produce one type of tunnel with square cross-section. However, in the tetragonal case, three-, four- and five-membered rings lead to tunnels of triangular, square and pentagonal cross-section. The tunnels only run in one dimension and the size of the A-type ion may limit its occupancy in the small channels. Similar stability criteria exist for both the bronze structures and the perovskites. Some of the related compounds of vanadium, molybdenum and niobium are more complicated than those of tungsten. Several of these, including a potassium molybdenum bronze, show a sheet rather than tunnel structure.

In the rutile (TiO_2) structure (Fig. 3c), the Ti atoms are in a body centred tetragonal formation with each atom surrounded by a slightly distorted octahedral arrangement of oxygen atoms. It is by both corner and edge sharing of these octahedra that a tunnel structure similar to ReO_3 is formed. Here the tunnels are one octahedron in width and length, extending infinitely in a direction parallel to the *c*-axis.

A rearrangement in the linking of the oxygen octahedra leads to other well-known structures. Ramsdellite has tunnels which are two octahedra wide and one long, whereas the tunnels of hollandite (Fig. 5) are two octahedra in both width and length. It is the hollandite structure ,which is therefore most able to accommodate atoms within its tunnels and may be a suitable structure for FIC. For many of the compounds found to exist with this type of structure there is a partial replacement of the transition element (usually

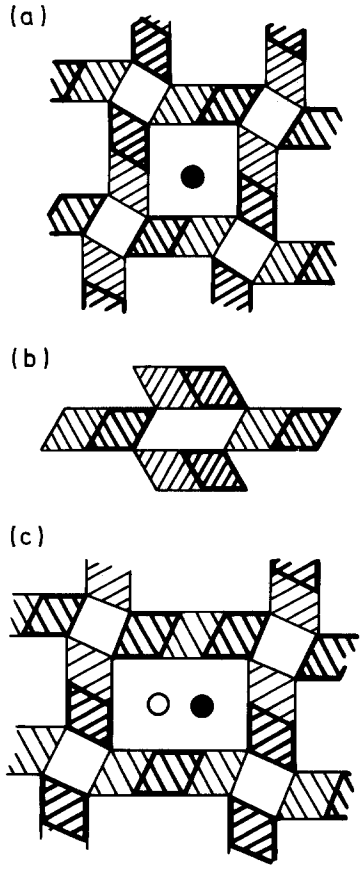

Figure 5 The structure of (a) hollandite (b) ramsdellite and (c) psilomelane, using the structural elements of Fig. 3. These structures may allow fast cation motion down the tunnels. After [129].

titanium) by other metals such as magnesium or aluminium. The ion most compatible in size with the typical width of the tunnels in hollandite is potassium, and this should travel along the channels with a low energy of migration. These compounds also exist over a wide range of stoichiometry which leads to low mobile ion site occupacy. Typical compounds have the form $A_xB_{x/2}Ti_{8-x/2}O_{16}$ with A an alkali or alkaline earth metal and B another metal. The range of x is typically $1.5 < x < 2.0$.

All of the structure types described above (discussed in greater detail in [129]), have parallel tunnels in one dimension only. This is a disadvantage from the viewpoint of ionic conduction since they may easily be blocked by impurity atoms, for example, which will impede ionic motion. The situation will clearly be helped by the presence of interconnections between the tunnels which will allow obstacles to be by-passed. We therefore need to find a material with a two- or three-dimensional interconnecting tunnel structure.

One group of compounds which exhibit such a three-dimensional structure is the hexacyanoferrates $A_2BFe(CN)_6$ with A an alkali metal and B a divalent alkaline earth or transition (post-transition) metal ion. The crystal structure is, in fact, a distorted perovskite, with alternating

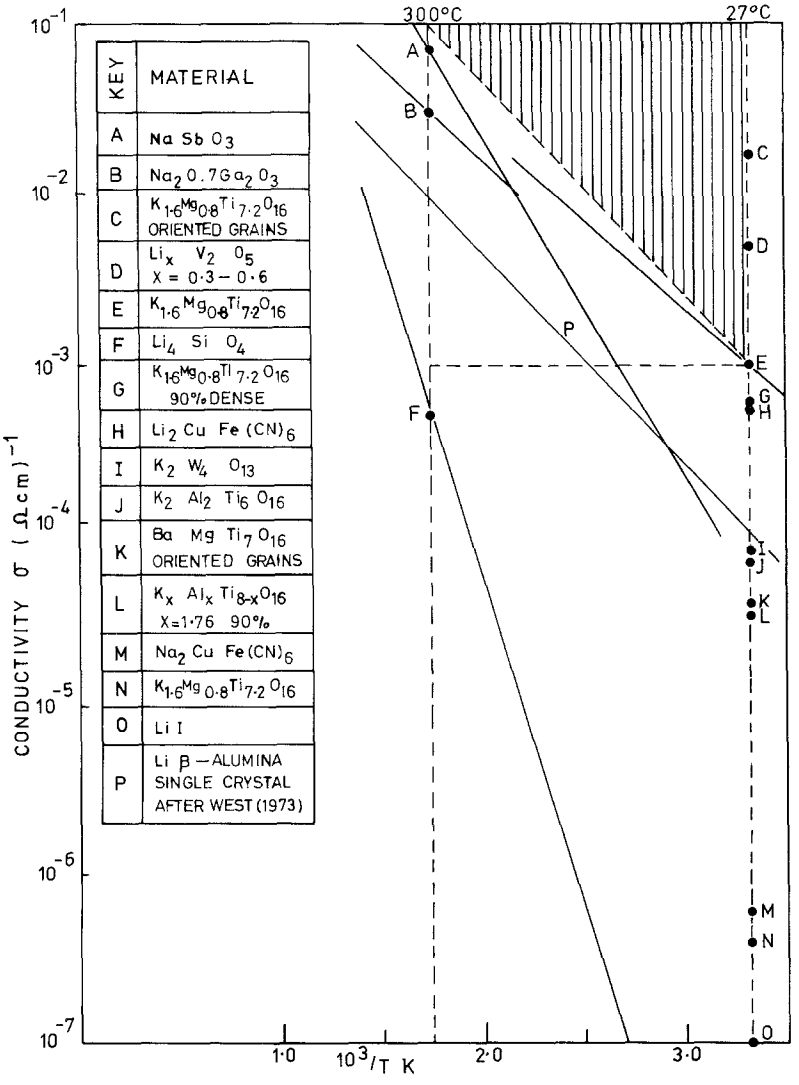

Figure 6 Graphical representation of some of the conducitivity data given in Table IV. Shaded area indicates the desirable conductivity region.

TABLE IV Alkali ion conductors

Material	Structure	σ (Ω^{-1} cm^{-1})	D (cm^2 sec^{-1})	E_A (eV)	t_e	Comments	Reference
$NaSbO_3$ polycrystalline 92% dense	SbO_3^- skeleton with alkali ions in tunnels along ⟨1 1 1⟩ axis. Cubic	$6-8 \times 10^{-2}$ at 300° C a.c. 1 kHz Aquadag and $NaNO_3$ electrodes		0.35		Ion exchanged from $KSbO_3$ 3-D tunnels – along ⟨1 1 1⟩ directions	[101, 102]
$NaSbO_3 . \frac{1}{6}$ NaF	Cubic	$5-8 \times 10^{-2}$ at 300° C		0.35		F atoms at intersections of ⟨1 1 1⟩ tunnels have little effect on σ	[101]
$NaTa_2O_5F$	Pyrochlore	$\sim 7 \times 10^{-3}$ at 300° C		0.4			[101]
$K_{1-x}Mg_{1-x}Al_{1+x}F_6$ $x = 0.1$		$\sim 2.5 \times 10^{-3}$ at 300° C		0.35			[101]
$Na_3Zr_2PSi_2O_{12}$	ZrO_6 octadera corner shared with SiO_4, PO_4 tetrahedra. Skeleton structure so formed has intersecting tunnels in which Na^+ reside and move	0.2 at 300° C		0.27		This compound has the highest conductivity in the system $Na_{1+x}Zr_2P_{3-x}Si_xO_{12}$ ($0 \leqslant x \leqslant 3$) and appears to be stable to molten sodium	[101]
Li_4SiO_4 and its solid solutions. Polycrystalline cold pressed and cold pressed plus 1000° C sinter (no change in properties)	3-D network of LiO_n polyhedra with triangular windows. Partial occupation of Li sites	$10^{-3} - 10^{-4}$ at 300° C ~ 1 at 700° C* Pt electrodes fixed with Au paste. For $\sigma < 10^{-2}$, 2 terminals and for $\sigma > 10^{-2}$, 4 terminals at 200 Hz–30 kHz				*Highest measured σ value was for compound $Li_4Si_xTi_{1-x}O_4$ with $x = 0.6$. σ values taken from the flattest portions of σ versus frequency plots	[103]
Li_2SiO_5		1.1×10^{-8} at 400° C		1.43		Complex plane a.c. conductivity plots allow the study of bulk and interfacial characteristics	[104, 105]
Li_2SiO_3		6.2×10^{-7} at 400° C		0.95			
Li_4SiO_4		9.0×10^{-4} at 400° C		0.78			
$LiAlSi_2O_6$	β-spodumene	1.4×10^{-5} at 400° C		0.95			
$LiAlSiO_4$	β-eucryptite	5.6×10^{-5} at 400° C		0.95			
	β-eucryptite glass ceramics	7×10^{-7} at 500 K 8×10^{-7} at 500 K		1.05 ~0.8			[106]
	glass	$\sim 2 \times 10^{-5}$ at 500 K		0.68			

TABLE IV (contd.)

$K_2Al_2Ti_6O_{16}$ polycrystalline 90% dense	Hollandite	$7.0 \mp 0.9 \times 10^{-5}$ at 300 K	0.265 ± 0.017		σ values are calculated from measurements of dielectric loss and subsequent Cole-Cole plots of ϵ' and ϵ''. This gives a so-called a.c. conductivity σ a.c. $\sigma_{ac} = (\epsilon_s - \epsilon_\infty)/T$ [13]
$K_{2x}Mg_xTi_{8-x}O_{16}$ $x = 0.8$ (a) 90% dense	Hollandite	$5.9 \pm 0.8 \times 10^{-4}$ at 300 K	0.21		
(b) ground from the reaction product (powder)		$4.2 \pm 0.7 \times 10^{-7}$ at 300 K	0.23 ± 0.017		
(c) partially oriented coarse grained ingot		$1.7 \pm 0.3 \times 10^{-2}$ at 300 K	0.22	$<5 \times 10^{-4}$	
$K_{2x}Al_{2x}Ti_{8-x}O_{16}$ $x = 0.88$ polycrystalline 90% dense	Hollandite	$3.5 \pm 0.6 \times 10^{-5}$ at 300 K	0.24	$<2.5 \times 10^{-6}$	
$BaMgTi_7O_{16}$ polycrystalline	Hollandite				T is a relaxation time and is *assumed* to be associated with space charge polarization due to mobile ions. Thus the attribution of σ_{ac} to ion transport is based on this assumption and is not directly proved
(a) ground from the reaction product (powder)		$1.9 \pm 0.3 \times 10^{-6}$ at 300 K	0.27 ± 0.017		
(b) 90% dense		$4.7 \pm 0.8 \times 10^{-5}$ at	0.25	$<2 \times 10^{-5}$	
(c) partially oriented coarse grained ingot		$4.2 \pm 0.8 \times 10^{-5}$ at 300 K	0.23	$<5 \times 10^{-5}$	
$K_xMg_{x/2}Ti_{8-x/2}O_{16}$ $x = 1.6$	Hollandite	σ values at extrapolations to 298 K 1×10^{-3} a.c. conductivity 300–1000 K 4×10^{-5} a.c. conductivity 300–500 K 2×10^{-4} dielectric loss 120–180 K			Time-dependent σ observed [107] and eliminated by preheating to above 700° C Below 300° C: frequency dependent σ even at 500 kHz Above 300° C' less frequency dependent. Increase in the electronic contribution* to the total σ. *Observed using a current pulse decay observation on a high frequency oscilloscope

TABLE IV (contd.)

Material	Structure	σ (Ω^{-1} cm^{-1})	D (cm^2 sec^{-1})	E_A (eV)	t_e	Comments	Referemce
						They claim good reproducibility of data but there is a very wide variation of σ values from within one technique (a.c. conductivity). See also [13] Electrodes are graphite or platinum in air atmosphere	[107]
$K_xMg_{x/2}Ti_{8-x/2}O_{16}$ $x = 1.6$	Hollandite					Large electronic contribution to the total conductivity is confirmed. See [107]	[37]
	Hollandite single crystal	4×10^{-3} at room temperature				Study on single crystal gave σ value at 10 kHz (galvanostatic). Potentiostatic results show motion to be short range	[108]
$K_2W_4O_{13}$ polycrystalline 95% dense	WO_3 octahedral linked tunnel structure	$8.3 \pm 1.0 \times 10^{-5}$ at 300 K		0.17 ± 0.017	>0.99	Electronic conduction predominates.	[13]
$Na_2Ti_6O_{13}$ polycrystalline coarse grained.						No dielectric loss peaks observed	[13]
LiI polycrystalline		$\sim 10^{-7}$ using a.c. 1 to 10 kHz at 300 K		~ 0.5			[109]
Li_2SO_4	fcc	1.04 at 600° C	4.2×10^{-5} at 750° C	σ: 0.40; D: 0.34		Temperature range studied (° C) 575–860	[110]
doped with mol % Ag_2SO_4							
17.5	fcc	1.0 at 550° C		0.43		524–570	
40	fcc	1.17 at 550° C		0.31		427–600	
50	bcc	1.17 at 550° C		0.31 (0.52 for D)		440–580	
60	bcc	1.1 at 550° C		0.3		462–560	
80		0.77 at 550° C		1.11		395–585	
90		0.12 at 550° C		1.5		486–640	
100		0.03 at 550° C		1.16		465–670	

TABLE IV (contd.)

mol % Na_2SO_4							
2	fcc	1.17 at 600° C		0.36		−867	[111]
4.9	fcc	1.08 at 600° C		0.36		−843	
10	fcc	1.22 at 600° C		0.34		466–754	
20	fcc	1.25 at 600° C		0.38		493–686	
30	fcc	1.2 at 600° C		0.33		474–650	
40	fcc	1.04 at 550° C		0.35		490–591	
40	bcc			0.35			
50	bcc	0.97 at 600° C		0.36(0.63 for D)		526–611	
70	hex	0.95 at 600° C		0.32		490–730	
80	hex	0.33 at 650° C		0.66		634–719	
90	hex	1.34 at 800° C		0.95		777–801	
100	hex	0.14 at 850° C		2.07		820–889	
$Li_{1+x}V_3O_8$ $x = 0.35$	Vanadium bronze		$D_0 \sim 10^{-8}$.nmr line-width 25–500° C	0.3			[112]
$Li_{1.1}V_3O_{7.9}$	bronze		10^{-17} at 300 K from nmr	0.3		Knight shift indicates appreciable electronic conduction	[113]
$Li_xV_2O_5$ $0.33 < x < 0.6$	bronze	10^2–10^3* at 300K. Four point a.c. cell e.m.f. for t_e values			0.96 at x = 0.33 0.09–0.45 at $x = 0.6$	*mixed conduction but σ values are contribution from ionic conduction only.	[114]
Hexacyanoferrates	3-D tunnels based on fcc structure					Preparative and structural information on other compounds with the general formula	[107]
$Na_2CuFe(CN)_6$	modified perovskite structure	6.10^{-7} at 300 K dielectric loss		0.48		$A'B''Fe(CN)_6$	
$Li_4Fe(CN)_6$				0.2 nmr		A'_2 = alkali or NH_4^+	
$(NH_4)_2Zn_3(CN)_6$				0.17 nmr		B'' = alkaline earth or transition metal	
$Li_2CuFe(CN)_6$				0.44, −55 to 55° C; 0.02, −74 to −117° C		Also: $A'_4Fe(CN)_6$ $A'B''Fe(CN)_6$ $B''_2Fe(CN)_6$ $B'''=Al^{3+}$	

TABLE IV (contd.)

Material	Structure	σ (Ω^{-1} cm^{-1})	D (cm^2 sec^{-1})	E_A (eV)	t_e	Comments	Reference
$Li_2CoFe(CN)_6$				0.044, −60 to −143° C nmr		nmr studies involve the plotting of linewidth ΔH_c in gauss against $1/T$K and calculating E_A from the gradient of the line $\Delta H_c = A \exp E_A/RT$	
$Na_2NiFe(CN)_6$				0.19 nmr		see [20]	
Hexacyanoferrates $A_2BFe(CN)_6$ compressed pellets	Distorted perovskite 3-D tunnels					A good correlation found between conductivity measurements and dielectric loss. Results from nmr motional narrowing studies are not in agreement however. May be due to the presence of paramagnetic ions. Electrical measurements: sputtered Pt electrodes gave σ largely independent of frequency. Vacuum conditions, *Highest value	[37]
$Li_2CuFe(CN)_6$		*6×10^{-4} at 313 K a.c. conductivity		0.28	~0		
$Li_2CuFe(CN)_6 5H_2O$		3×10^{-5} at 295 K a.c. conductivity		0.50			
$Na_2CuFe(CN)_6$		5×10^{-7} at 295 K a.c. conductivity		0.51	0.08		
$Na_2CuFe(CN)_6$		6×10^{-7} at 295 K Dielectric loss		0.505			[37]
$Na_2MgFe(CN)_6$		3×10^{-6} at 295 K		0.49	0.39		
$Na_2NiFe(CN)_6$		3×10^{-6} at 295 K a.c. conductivity		0.40	0.61		
Lithium titanium oxides, in particular $Li_2Ti_xO_{2x+1}$ with $x = 1, 2, 3$.	Li_2TiO_3 : NaCl type $Li_2Ti_2O_5$: spinel $Li_2Ti_3O_7$: ramsdellite	0.1 at 500 K		0.5		nmr results show E_A ~ 0.15 eV for Li_7 : thought to be rattling in the lattice	[107] [104]
$KAlF_4$ doped with: (a) ZrF_4 (b) BaF_2 *AlF_3 (c) undoped Polycrystalline and single crystal	Tetragonal layered structure	a.c. sputtered Pt electrodes in vacuum log σ against $1/T$ curves are two stage: intrinsic and extrinsic, 10^{-5} to 10^{-6} at 300° C at 6 kHz			small	Complex admittance techniques used	[37]

TABLE IV (contd.)

$LiAl_2O_2$ polycrystalline	Rock-salt at low temperature. Above 900° C cation disordered phase	6×10^{-5} at 700° C Sputtered Au electrodes in air. 10 kHz a.c.		0.6	0.02	σ is frequency dependent and complex admittance analysis indicate that this is not the true bulk value of conductivity	[37]
$LiAlGeO_4$ polycrystalline	Phenacite < 1000° C	2.7×10^{-5} at 1000 K Sputtered Pt electrodes in air a.c. 10 kHz		0.9	0.15 at 1000 K	d.c. (electronic) conductivity at 1000 K is 3.9×10^{-6} Ω^{-1} cm^{-1} with E_A of 1.42 eV. nmr linewidth at 298 K is 1.98 G indicates fairly rapid motion of Li^+ but does not distinguish between long range and localized motion	[37]
Li_2GeO_3	Unknown	3×10^{-5} at 500 K		1.0			[104]
$Li_6Ge_8O_{19}$	Probably not ramsdellite	6×10^{-5} at 500 K		0.56			
$Li_2Ge_7O_{15}$	Unknown	10^{-7} at 500 K		0.93			
$K_xNa_{1-x}Fe_7O_{11}$	Similar to β-alumina structure of $KFe_{11}O_{17}$		$D_{self}10^{-5}$-10^{-6} at 300° C 2.6×10^{-8} at 300 K radiotracer diffusion	0.1–0.2 dielectric loss. 0.3–0.5 tracer diffusion		(a) E_A (tracer) > E_A (dielectric loss) (b) D (room temperature) as measured is greater than expected value from an extrapolation of higher temperature results. Both (a) and (b) suggest a different activation energy for high and low temperatures. Lower E_A at lower temperatures.	[115]
K_2O:Li_2O:TiO_2 system $K_xLi_xTi_{4-x/2}$ in particular	Tunnels. Evidence of hollandite and ramsdellite structure in the general system					Li ions exist both within the tunnels and substitutionally on Ti sites	[128]
$Na_xFe_xTi_{2-x}O_4$ $0.9 > x > 0.75$ powder	Double parallel tunnels					$NaFeTiO_4$ is isomorphous with a whole range of compounds $NaA^{3+}B^{4+}O_4$	[117]

TABLE IV (contd.)

Material	Structure		σ (Ω^{-1} cm^{-1})	D (cm^2 sec^{-1})	E_A (eV)	t_e	Comments	Reference
General system $A^+B^{5+}O_3$ B = Nb, Ta, Sb and Bi							General look at the structure and bonding found in these compounds Possibly open enough for rapid ion motion	[118]
Li_3AlN_2 Li_3BN_2 $Li_xTa_2O_5$ $Li_xV_2O_5$ $NaPrF_4$ $NaYbF_4$ $LiNb_6O_{15}F$ $LiNO_3$ Zeolite Hollandites Cordierites Tungsten bronzes $Li_2Ge_7O_{15}$ $Li_2Ge_7O_9$ $NaLaF_4$ (La = lanthanum or yttrium) Dalytite ($K_2ZrSi_6O_{15}$) Defect perovskites	Glass Glass						Final report of study of solid cationic conductors (June 1972), published November 1973. nmr Pulsed conductivity Microwave conductivity Dielectric loss d.c. conductivity None of the material studied showed (high) long-range conductivity values. Evidence of "rattling" from nmr etc. Recommends study of 2- and 3-D interconnected channel structures only. Suggests some small channel zeolites as possible candidates.	[119]
Alkali oxide/metal oxide systems		*Tunnel size (co-ordination)*						
Li_2O, Na_2O, K_2O with Ta_2O_5 or Nb_2O_5	Tunnel						Preparative information, no σ or D data	[116]
$Li_2O_{14}Nb_2O_5$	N-Nb_2O_5	4-fold					FIC possible from structural considerations	
$5Li_2O.95Ta_2O_5$	L-Ta_2O_5	3						
$LiTa_5MoO_{16}$	$LiNb_6O_{15}F$	4						

TABLE IV (contd.)

$Na_2O.3Ta_2O_5$ – $Na_2O.4Ta_2O_5$	Tetragonal tungsten bronze	4 & 5					
$H.K_2O\ 2Ta_2O_5$	Tetragonal tungsten bronze	4 & 5					
$H.K_2O\ 5Ta_2O_5$	Tetragonal tungsten bronze	4 & 5					
$2K_2O\ 7Ta_2O_5$	Hexagonal bronze	6					
$K_2O\ 8Ta_2O_5$ typically	Rb-niobate	4, 6 & 7					
Graphite intercalation compounds Graphite/CrO_3 : Graphite/phosphoric acid CrO_3 : Graphite/SbF_5	Layer						Some nmr work. No concrete data. Mixed conductor cathode material? [107]
Na-Graphite-CrO_3 and related interstitial compounds	Layer			$D_0 \sim 10^{-6}$ estimate only for Na-graphite-CrO_3			Mixed conductivity. Use as cathode? [120]
Micas, e.g. Muscovite (Na) Paragonite (K) (Aluminoscilicates)	Layer						Some (ion exchange) evidence for fast ionic motion between layers (2-dimensional) [55]
Silicate glass			10^{-3} at 450° C 10^{-7} at 25° C Au or Pt electrodes a.c.			Zero	[121]
Fused silica					~ 1.0		Activation energy for Na^+ or K^+ ions [122]

TABLE IV (contd.)

Material	Structure	σ (Ω^{-1} cm^{-1})	D (cm^2 sec^{-1})	E_A (eV)	t_e	Comments	Reference
Zeolites: (a) Analcites $M_2OAl_2O_3 4SiO_2$			at 25° C Na^+: 10^{-13} * Cs^+: 10^{-24} *	Na^+ 0.5 K^+ 0.7 Rb^+ 0.8 Cs^+ 1.1		*Krypton BET absorpton technique †Geometrical area technique $D^\dagger$ is $\neq D^*$ $D^\dagger$ may be $10^6 D^*$. Therefore any value obtained by * is falsely low	[123]
(b) Chabazite $M_2OAl_2O_3$ 6.74 SiO_2 $6H_2O$ typically			at 250° C Na^+: 10^{-8} † Rb^+: 10^{-8} † K^+: 4 10^{-8} † Cs^+: 10^{-9} †	Na^+ 0.5 K^+ 0.3 Rb^+ 0.25 Cs^+ 0.3 Ca^{2+} 0.6 Sr^{2+} 0.6 Ba^{2+} 0.4			

B and Fe ions at cube corners and face centres leading to a superlattice structure. The CN^- ions form the tunnel walls.

In addition to this group of compounds, many other single materials (e.g. $NaSbO_3$, $Na_xFe_xTi_{2-x}O_4$) are found to exist with multi-dimensional tunnel structures, which are distortions of the previously described octahedral configurations. Other materials falling into the category, and particularly investigated by Goodenough *et al.* [101] are materials of the pyrochlore structure (which are well known to ion exchange) and the analogues of $NaSbO_3$ [118]. One particular compound of interest is $Na_3Zr_2PSi_2O_{12}$, which is stable to molten sodium and has conductivity comparable to β–Al_2O_3 in the important temperature range. This compound has corner shared oxygen octahedra and tetrahedra with some sodium ions octahedrally co-ordinated to oxygen at the intersection sites of continuous networks of three-dimensional tunnels. Other sodium ions reside along the tunnels, whose minimum diameter bottleneck is large enough to allow ready diffusion of the ions. This material, known colloquially as "nazirpsio", has stimulated a great deal of interest. It competes directly with beta-alumina at the operating temperature of the sodium–sulphur battery, and appears to have the required chemical stability. Furthermore, it indicates to those involved in the search for new materials that careful application of the principles of structural chemistry can bring its reward.

Solid electrolytes based on lithium sulphate have been a fruitful area of research. Kvist, Lunden and co-workers have studied ionic conductivity and diffusion in a wide range of solid solutions, and a representative collection of data is presented in Table IV. Lithium sulphate itself has a phase change to a highly conducting f c c structure at 572°C in which there are three available sites per cation. There is appreciable conductivity of $\sim 1\ \Omega^{-1}\ cm^{-1}$ at 600°C, and only a slight increase in conductivity when the compound melts at 860°C. Some of these electrolytes have been incorporated in small cells [124]. These materials and their high conductivity, should provide a precedent to encourage workers to examine other apparently simple materials for anomalously high ionic conductivity.

9. Conclusion

This review has attempted to present a comprehensive compilation of currently available FIC data. In the case of the alkali ion conductors, discouraging data on a number of materials is listed, whilst others are essentially speculative suggestions. It seems likely that the discovery of new materials will continue on this *ad hoc* and partly empirical basis, but steady progress over the next few years should produce a greater degree of understanding and consequently a better insight into the properties required for improved fast ion conductivities.

Acknowledgements

We would like to thank Drs A.E. Hughes and B.C. Tofield for stimulating discussions.

References

1. R. A. HUGGINS, in "Diffusion in Solids: Recent Developments", edited by A.S. Nowick and J.J. Burton (Academic Press, London, 1975).
2. B. C. H. STEELE and G. J. DUDLEY, in "International Review of Science: Inorganic Chemistry Series Two", Vol. 10, Solid State Chemistry, edited by L.E.J. Roberts (Butterworths, London, 1975).
3. J. HLADIK, "Physics of Electrolytes", Vols. 1 and 2 (Academic Press, New York, 1975).
4. W. VAN GOOL, Ed. "Fast Ion Transport in Solids" (Plenum, New York, 1973).
5. *Idem, Rev. Mater. Sci.* **4** (1974) 311.
6. M. S. WHITTINGHAM and R. A. HUGGINS, *J. Chem. Phys.* **54** (1971) 414.
7. *Idem, J. Electrochem. Soc.* **118** (1971) 1.
8. D. S. DEMOTT and P. HANCOCK, *Proc. Brit. Ceram. Soc.* **19** (1971) 193.
9. R. D. ARMSTRONG, T. DICKINSON and R. WHITFIELD, *J. Electroanal. Chem.* **39** (1972) 257.
10. R. W. POWERS and S. P. MITOFF, *J. Electrochem. Soc.* **122** (1975) 226.
11. J. T. KUMMER, *Progr. Solid State Chem.* **7** (1972) 141.
12. Y. Y. YAO and J. T. KUMMER, *J. Inor. Nucl. Chem.* **29** (1967) 2453.
13. J. SINGER, H. E. KAUTZ, W. L. FIELDER and J. S. FORDYCE, in [4], p. 653.
14. A. K. JONSCHER, *Nature* **253** (1975) 717.
15. A. IMAI and M. HARATA, *Jap. J. of Appl.* **Phys. 11** (1972) 180.
16. S. P. MITOFF and R. T. CHARLES, *J. Appl. Phys.* **43** (1972) 927.
17. J. W. PATTERSON, E. C. BOGREN and R. A. RAPP, *J. Electrochem. Soc.* **114** (1967) 752.
18. A. V. JOSHI and J. B. WAGNER, *ibid,* **122** (1975) 1071.
19. G. C. FARRINGTON, *ibid,* **121** (1974) 1314.

20. T. G. STOEBE and R. A. HUGGINS, *J. Mater. Sci.* **1** (1966) 117.
21. I. CHUNG, PhD Thesis, State University of New York 1974: Microfilm 75-2341; I. CHUNG and H. STORY, *J. Chem. Phys.* **63** (1975) 4903.
22. J. P. BOILOT, L. ZUPPIROLI, G. DELPLANQUE and L. JEROME, *Phil. Mag.* **32** (1975) 343; D. JEROME and J. P. BOILOT, *J. Phys.* **35** (1974) L129.
23. J. ANTOINE, D. VIVIEN, J. LIVAGE, J. THERY and R. COLLONGUES, *Mat. Res. Bull.* **10** (1975) 865.
24. W. L. ROTH, *Trans. Amer. Cryst. Assoc.* **11** (1975) 51.
25 C. A. BEEVERS and M. A. S. ROSS, *Z. Kristallogr.* **97** (1937) 59.
26. W. L. ROTH, *J. Solid State Chem.* **4** (1972) 60.
27. J. S. KASPER and K. W. BROWALL, *ibid.*, **13** (1975) 49.
28. S. J. ALLEN and J. P. REMEIKA, *Phys. Rev. Letters* **33** (1974) 1478.
29. R. D. ARMSTRONG, P. M. A. SHERWOOD and R. A. WIGGINS, *Spectrochimica Acta* **30A** (1974) 1213.
30. R. T. HARLEY, W. HAYES, A. J. RUSHWORTH and J. F. RYAN, *J. Phys. C.* **8** (1975) L530.
31. S. CHANDRA and V. K. MOHABEY, *J. Phys.* **D8** (1975) 576.
32. K. S. COLE and R. H. COLE, *J. Chem. Phys.* **9** (1941) 341.
33. J. E. BAUERLE, *J. Phys. Chem. Solids* **30** (1969) 2657.
34. E. SCHOULER, M. KLEITZ and C. DEPORTES, *Chem. Phys.* **70** (1973) 923, 1309.
35. R. D. ARMSTRONG *et al.*, *J. Electroanal. Chem.* **53** (1974) 389.
36. R. D. ARMSTRONG and K. TAYLOR, *ibid.*, **63** (1975) 9.
37. R. A. HUGGINS, Stanford Res. Rept. No AD-782 365 (1974).
38. R. A. HUGGINS, Stanford Res. Rept. No AD-A012 098 (1975).
39. J. R. MACDONALD, *J. Chem. Phys.* **61** (1974) 3977.
40. R. J. FRIAUF, [3], p. 1103.
41. H. RICKERT, [4], p. 33.
42. R. D. ARMSTRONG, R. S. BULMER and T. DICKINSON, [4], p. 269.
43. K. W. BROWALL and J. S. KASPER, *J. Solid State Chem.* **15** (1975) 54.
44. B. B. OWENS, [4], p. 593.
45. S. GELLER, in [4], p. 607.
46. J. N. BRADLEY and P. D. GREENE, *Trans. Farad. Soc.* **63** (Part 10) (1967) 2516 and reference therein
47. C. C. LIANG, in [4], p. 19.
48. D. KUNZE, in [4], p. 405.
49. T. TAKAHASHI, S. IKEDA and O. YAMAMOTO, *J. Electrochem. Soc.* **119** (1972) 477.
50. *Idem, ibid.*, **120** (1973) 647.
51. S. GELLER, and P. M. SKARSTAD, *Phys. Rev. Letters* **33** (25) (1974) 1484.
52. S. GELLER, P. M. SKARSTAD and S. A. WILBER, *J. Electrochem. Soc.* **122** (1975) 322.
53. K. SHAHI and S. CHANDRA, *J. Phys. C.* **8** (1975) 2255.
54. B. SCROSATI, F. PAPALEO and G. PISTOIA, *J. Electrochem. Soc.* **122** (1975) 339.
55. W. VAN GOOL, in [4], p. 201.
56. L. W. STROCK, *J. Phys. Chem.* **B25** (1934) 441; *J. Phys. Chem.* **B31** (1935) 132.
57. J. H. CHRISTIE, B. B. OWENS and G. T. TREDEMAN, *Inorg. Chem.* **14** (1975) 1423.
58. R. G. LINFORD, J. M. POLLOCK and C. F. RANDELL, *Nature* **256** (1975) 398.
59. A. F. SAMMELS, J. Z. GUOGOUTAS and B. B. OWENS, *J. Electrochem. Soc.* **122** (1975) 1291.
60. T. H. ESTELL and S. N. FLENGASS, *Chem. Rev.* **70** (1970) 339.
61. T. TAKAHASHI, H. IWAHARA and J. NAGAI, *J. Appl. Electrochem.* **2** (1972) 97.
62. T. TAKAHASHI and H. IWAHARA, *ibid.*, **3** (1973) 65.
63. T. TAKAHASHI, H. IWAHARA and T. ARAO, *ibid.*, **5** (1976) 187.
64. T. TAKAHASHI, T. ESEKA and H. IWAHARA, *ibid.*, **5** (1975) 197.
65. M. KLEITZ, in [4], p. 607.
66. W. BAUKEL, "From Electrocatalysis to Fuel Cells", edited by G. Stansted, (University of Washington Press, 1971) p. 345.
67. C. E. DERRINGTON and M. O'KEEFFE, *Solid Commun. 15* (1974) 1175.
68. C. E. DERRINGTON, A. LINDNER and M. O.-KEEFFE, *J. Solid State Chem.* **15** (1975) 171.
69. German Patent Application 2401 497.
70. J. KORYTA, "Ion Selective electrodes" (Cambridge University Press, 1975).
71. L. E. NAGEL and M. O'KEEFFE, in [4], p. 165.
72. J. BRUININK, *ibid.*, p. 157.
73. A. F. WELLS, "Structural Inorganic Chemistry", 3rd Edn. (Clarendon Press, Oxford, 1962) p. 305.
74. T. DOSDALE, D. E. C. CORBRIDGE and R. J. BROOK, private communication (1975).
75. P. G. DICKENS, D. J. MURPHY and T. K. HALSTEAD, *J. Solid State Chem.* **6** (1973) 370.
76. W. VAN GOOL and P. H. BOTTELBERGHS, *ibid.*, **7** (1973) 59.
77. H. SATO and R. KIKUCHI, *J. Chem. Phys.* **55** (1971) 677.
78. M. J. RICE and W. L. ROTH, *J. Solid State Chem.* **4** (1972) 294.
79. D. R. FLINN, N. McDONOUGH, K. H. STERN and R. RICE, *Electrochem. Soc. Ext. Abs.* **75-1**, p. 23.
80. L. J. MILES and I. WYNN JONES, *Proc. Brit. Ceram Soc.* **19** (1971) 161.
81. *Idem, ibid.*, **19** (1971) 179.
82. R. D. ARMSTRONG, T. DICKINSON and J. TURNER, *J. Electrochem. Soc.* **118** (1971) 1135.
83. R. D. ARMSTRONG *et al.*, *Electrochim Acta* **19** (1974) 187.
84. R. D. ARMSTRONG, T. DICKINSON and P. M. WILLIS, *J. Electroanal. Chem. and Interfacial Electrochem.* **53** (1974) 389.
85. L. HSUEH and D. N. BENNION, *J. Electrochem. Soc.* **118** (1971) 1128.

86. R. A. HUGGINS, Stanford University Technical Reports AD 773972, 782365.
87. B. V. JOQLEKAR, P. S. NICHOLSON and W. W. SMELTZER, *Canad. Met. Q.* **12** (1973) 155.
88. H. McGOWAN, Ph.D. Thesis, State University of New Jersey, USA (1973).
89. A. D. MORRISON, R. W. STORMONT and F. H. COCKS, *J. Amer. Ceram. Soc.* **58** (1975) 41.
90. R. W. POWERS and S. P. MITOFF, *J. Electrochem. Soc.* **122** (1975) 226.
91. R. H. RADZILOWSKI, Y. F. YAO and J. T. KUMMER, *J. Appl. Phys.* **40** (1969) 4716.
92. R. H. RICHMAN and G. J. TENNENHOUSE, *J. Amer. Ceram. Soc.* **58** (1975) 63.
93. R. STEVENS, *J. Mater. Sci.* **9** (1974) 801.
94. *Idem, ibid.*, **9** (1974) 934.
95. C. T. H. STODDART and E. D. HONDROS, *J. Brit. Ceram. Soc.*, **73** (1974) 61.
96. N. WEBER, *Energy Conversion* **14** (1974) 1.
97. M. S. WHITTINGHAM and R. A. HUGGINS, Nat. Bur. of Stand. Special Publ. 364. Sol St. Chem. Proc. of 5th Res. Symp. (1972).
98. R. T. CHICOTKA, *Electrochem. Soc. Ext. Abs.* 75-1, p. 16.
99. L. M. FOSTER and J. E. SCARDEFIELD, *ibid.*, 75-1, p. 14.
100. G. J. DUDLEY and B. C. H. STEELE, private communication (1975).
101. J. B. GOODENOUGH, H. Y-P. HONG and J. A. KAFALAS, *Mat. Res. Bull.* **11** (1976) 203.
102. H. Y-P. HONG, J. A. KAFALAS and J. B. GOODENOUGH, Lincoln Lab (MIT), Sol. State Res. Rep. (1974).
103. A. R. WEST, *J. Appl. Electrochem.* **3** (1973) 327.
104. R. A. HUGGINS, "Solid Electrolyte Battery Materials", Report AD-A012 098 (1975).
105. I. D. RAISTRICK, L. A. NAGEL and R. A. HUGGINS, *Electrochem. Soc. Est. Abs.* 75-1, p. 50.
106. R. T. JOHNSON, Jr., B. MOROSIN, M. L. KNOTEK and R. M. BIEFELD, *Phys. Letters* **54A** (1975) 403.
107. R. A. HUGGINS, Stanford University Tech. Rep. AD 773 972, (1973).
108. G. C. FARRINGTON, *Electrochem. Soc. Ext. Abs.* 75-1, p. 48.
109. C. R. SCHLAIKJER, and C. C. LIANG, in [4], p. 685.
110. A. KVIST, *Z. Naturforsch.* **22a** (1967) 208.
111. A. M. JOSEFSON and A. KVIST, *ibid.*, **24a** (1969) 466.
112. M. S. WHITTINGHAM and R. A. HUGGINS, in [4], p. 645.
113. T. K. HALSTEAD, W. U. BENECH, R. D. GULLIVER II. and R. A. HUGGINS, *J. Chem. Phys.* **58** (1973) 3530.
114. S. P. MITOFF in [4], p. 415.
115. K. O. HEVER, *J. Electrochem. Soc.* **115** (1968) 826.
116. R. S. ROTH, H. S. PARKER, W. S. BROWER and J. L. WARING, in [4], p. 217.
117. W. G. MUMME and A. F. REID, *Acta Cryst.* **B24** (1968) 625.
118. J. B. GOODENOUGH and J. A. KAFALAS, *J. Sol. State Chem.* **6** (1973) 493.
119. W. L. ROTH *et al.* Final Rep. N74-26498 (NASA, CR-124610) (April 1974).
120. M. B. ARMAND, in [4], p. 665.
121. I. RAVEIN, private communication (1974).
122. K. H. STERN, in [4], p. 393.
123. L. V. C. REES, *ibid.*, p. 301.
124. B. HEAD, A. LUNDEN and K. SÇHROEDER, *Proc. IECEC* (1975) 613.
125. A. ABRAGAM, "The Principles of Nuclear Magnetism" (Clarendon Press, Oxford, 1961) p. 327.
126. A. D. LECLAIRE, in [4], p. 51.
127. W. L. ROTH, General Electric Tech. Inf. Series, Schenectady, N.Y. Rep. No. 74CRD054 (March 1974).
128. R. S. ROTH, H. S. PARKER and W. S. BROWER, *Mat. Res. Bull.* **8** (1973) 327.
129. P. G. DICKENS and P. J. WISEMAN, in "International Review of Science: Inorganic Chemistry Series Two", Vol. 10, Solid State Chemistry, edited by L.E.J. Roberts (Butterworths, London, 1975).
130. D. B. McWHAN, S. M. SAHPIRO, J. P. REMEIKA and G. SHIRANE, *J. Phys. C.* **8** (1975) L487.
131. H. FUESS, K. FUNKE and J. KALUS, *Phys. Stat. Sol. (a)* **32** (1975) 101.
132. G. ECKOLD, K. FUNKE, J. KALUS and R. E. LECHNER, *Phys. Letters* **55A** (1975) 125.
133. T. KODAMA and G. MUTO, *J. Solid State Chem.* **17** (1976) 61.
134. D. B. McWHAN, S. J. ALLEN, Jun., J. P. REMEIKA and P. D. DERNIER, *Phys. Rev. Letters* **35** (1975) 953.
135. M. NAGAO and T. KANEDA, *Phys. Rev.* **B11** (1975) 2711.
136. J. C. WANG, M. GAFFARI and SANG-IL CHOI, *J. Chem. Phys.* **63** (1975) 772.

Received 5 March and accepted 28 May 1976.